

Online Supplementary Material for:

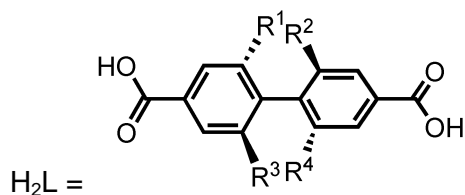
**Influence of sterically non-hindering methyl groups on adsorption
properties of two classical zinc and copper MOF types**

Ishtvan Boldog^a, Lei Xing^a, Axel Schulz^b, Christoph Janiak^{a,*}

^a Institut für Anorganische Chemie und Strukturchemie, Universität Düsseldorf,
Universitätsstr. 1, D-40225 Düsseldorf, Germany

^b Institut für Chemie, Abteilung Anorganische Chemie, Universität Rostock, Albert-Einstein-
Str. 3a, D-18059 Rostock, Germany

Table S1 MOFs with known structure based on 4,4'-biphenyldicarboxylates with at least one non-H *meta*-substituent, with a condition that the substituent should not be a carboxylate group and that no bonds between the substituents are allowed.^a



R ¹ , R ² , R ³ , R ⁴	Comment	Reported properties or transformations	Ref. Doi (dx.doi.org/...)
NO ₂ , NO ₂ , H, H	3D mixed ligand (with 1,3-dipyrid-4-yl-propane) coordination polymers of Mn, Co, Ni, Cd [ML(phen)], M = Co, Ni, Zn, 3D mixed ligand MOFs 3D mixed ligand (with 1,3-diimidazol-4-ylalkanes) coordination polymers of Mn, Co, Cu, Zn, Cd	Magnetism Magnetism Magnetism	B. Li, G. Li, D. Liu, Y. Peng, X. Zhou, J. Hua, Z. Shi, S. Feng, CrystEngComm 13 (2011) 1291-1298. 10.1039/c0ce00252f J.-Y. Zhang, Y. Ma, A.-L. Cheng, Q. Yue, Q. Sun, E.-Q. Gao, Dalton Trans. 40 (2011) 7219–7227. 10.1039/c1dt10158g B. Li, X. Zhou, Q. Zhou, G. Li, J. Hua, Y. Bi, Y. Li, Z. Shi, S. Feng, CrystEngComm 13 (2011) 4592-4598. 10.1039/c1ce05061c
2-NHR, H, H, H R = H, COOtBu	Non-interpenetrated [Zn ₄ OL ₃] IRMOF	Postsynthetic modification by thermally induced cleavage of Boc protecting group	R. K. Deshpande, J. L. Minnaar, S. G. Telfer, Angew. Chem. Int. Ed. 49 (2010) 4598-4602. 10.1002/anie.200905960
Me, Me, OH, OH	Non-interpenetrated [Cu ₂ L ₂] · Guest, nbo network	Catalytic enantioselective carbonyl-ene and Diels-Alder reactions (removal of guest without framework collapse molecules was not achieved)	K. S. Jeong, Y. B. Go, S. M. Shin, S. J. Lee, J. Kim, O. M. Yaghi, N. Jeong, Chem. Sci. 2 (2011) 877-882. 10.1039/c0sc00582g
R, H, H, H R = CHO, C=N-NH-2,4-C ₆ H ₄ (NO ₂) ₂ , OMe	Doubly-interpenetrated [Zn ₄ OL ₃] IRMOF	Postsynthetic modification (hydrazone formation) and mixed ligand IRMOFs. Interpenetration control	A. D. Burrows, C. G. Frost, M. F. Mahon and C. Richardson, Angew. Chem. Int. Ed. 47 (2008) 8482-8486. 10.1002/anie.200802908
Me, Me, Me, Me	Non- and doubly interpenetrated [Zn ₄ OL _{3-x} L _x ^{2-x}] IRMOF	Mixed ligand IRMOFs, interpenetration control	T.-H. Park, K. Koh, A. G. Wong-Foy, A. J. Matzger, Cryst. Growth Des. 11 (2011) 2059-2063. 10.1021/cg200271e

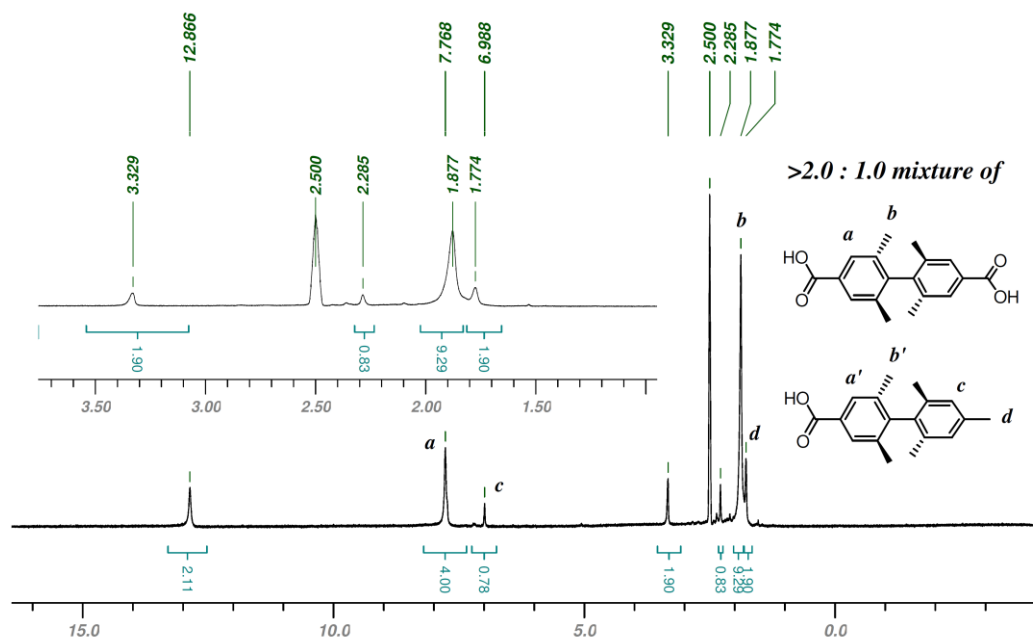
CN, CN, H, H Me, Me, H, H I, I, H, H	[Cu ₂ L ₂] · Guest, NbO network	Demonstration of network design possibilities, Selective adsorption studies	H. Furukawa, J. Kim, N. W. Ockwig, M. O’Keeffe, O. M. Yaghi, J. Am. Chem. Soc. 130 (2008) 11650-11661. 10.1021/ja803783c
CH ₂ SMe, H, H, H CH ₂ SO ₂ Me, H, H, H	Doubly-interpenetrated [Zn ₄ OL ₃] IRMOF	Postsynthetic modification of (sulfide to sulfone).	A. D. Burrows, C. G. Frost, M. F. Mahon and C. Richardson, Chem. Commun. (2009) 4218-4220. 10.1039/b906170c

^a Cambridge Structure Database search, version 5.33, November 2011. Not shown in the Table are the cases, when R= COOH, or an R-R linkage is present.

Synthesis

2,2',6,6'-tetramethyl-4,4'-biphenyldicarboxylic acid, H₂Me₄BPDC, **1**:

IBD220_10h, the crude product after washings and drying on air, in DMSO-d₆



2,2',6,6'-tetramethyl-4,4'-biphenylcarboxylic acid in DMSO-d₆

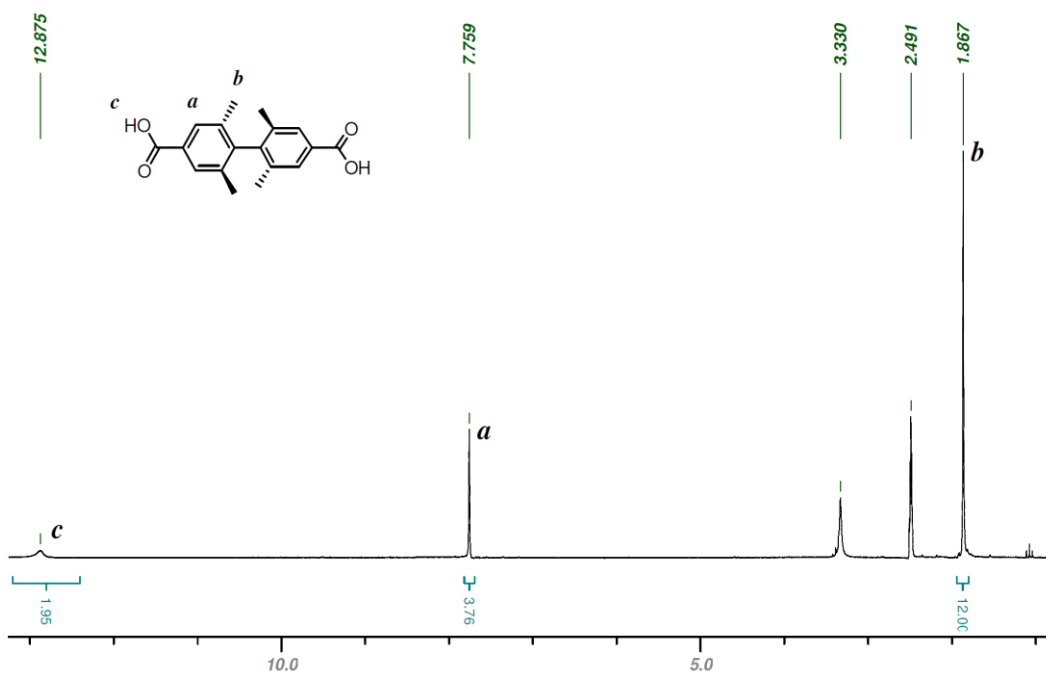


Fig. S1 ¹H NMR spectra of the crude reaction mixture of H₂Me₄BPDC and 4-(2,4,6-trimethylphenyl)-3,5-dimethylphenylcarboxylic acid with a molar ratio of about 2.1:1.0 (above) and the pure H₂Me₄BPDC (below, crop from the first extraction).

Thermogravimetric - differential thermal analysis (TG-DTA)

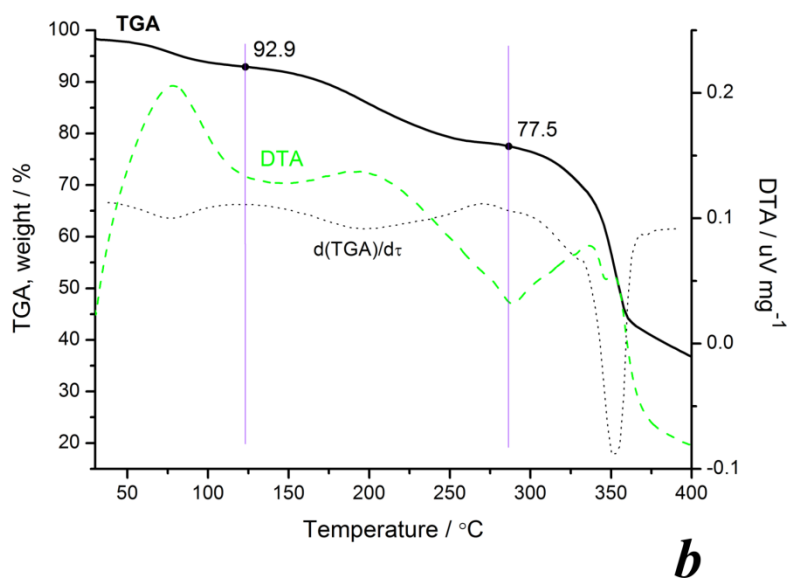
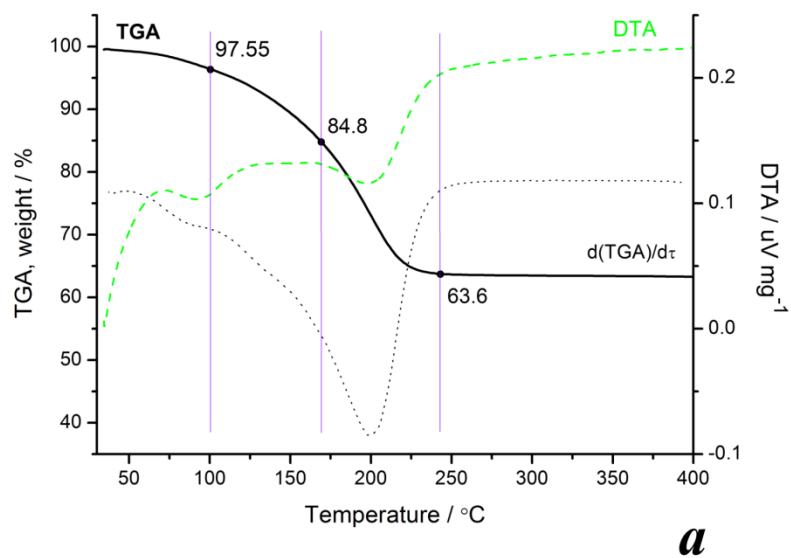


Fig. S2 TG-DTA for **2** · 9 DMF (as synthesized) and **3** (after degassing of the partially solvent-exchanged **3** · 9 DMF)

Infrared (IR) spectra

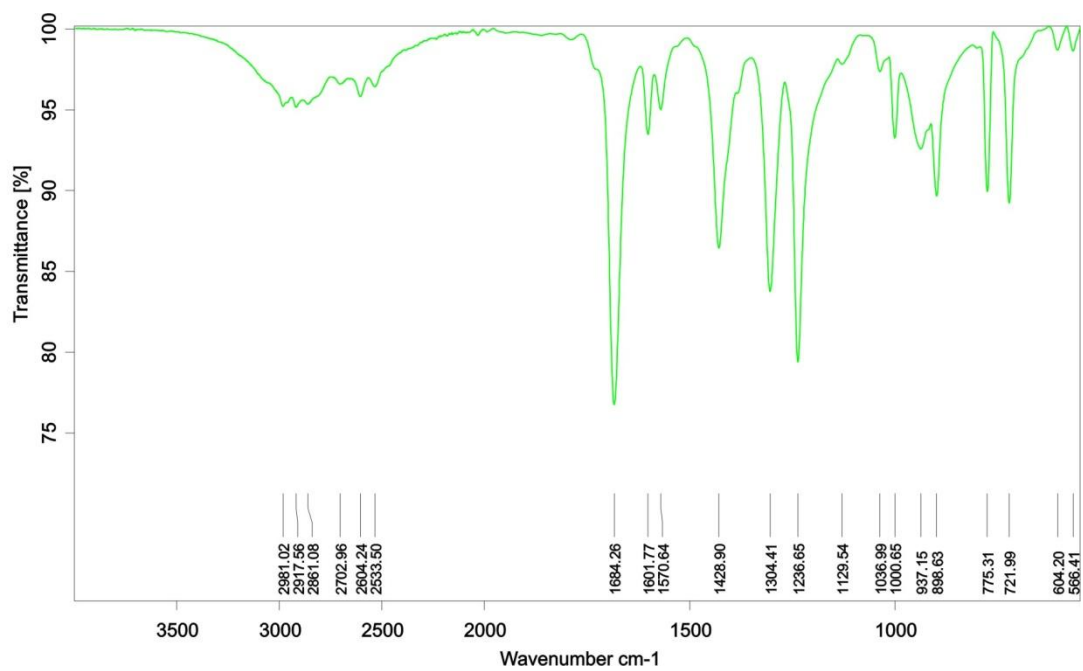


Fig. S3 IR spectrum of H₂Me₄BPDC

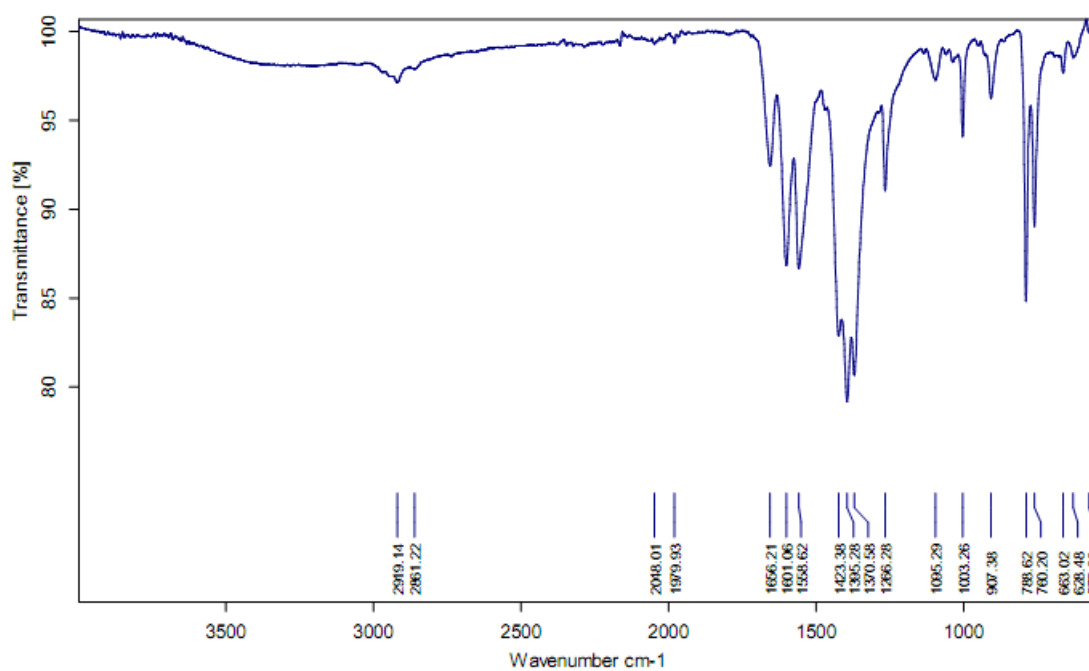


Fig. S4 IR spectrum of $[\text{Zn}_4\text{O}(\text{Me}_4\text{BPDC})_3] \cdot 9 \text{ DMF}, \mathbf{2} \cdot 9 \text{ DMF}$, (as synthesized).

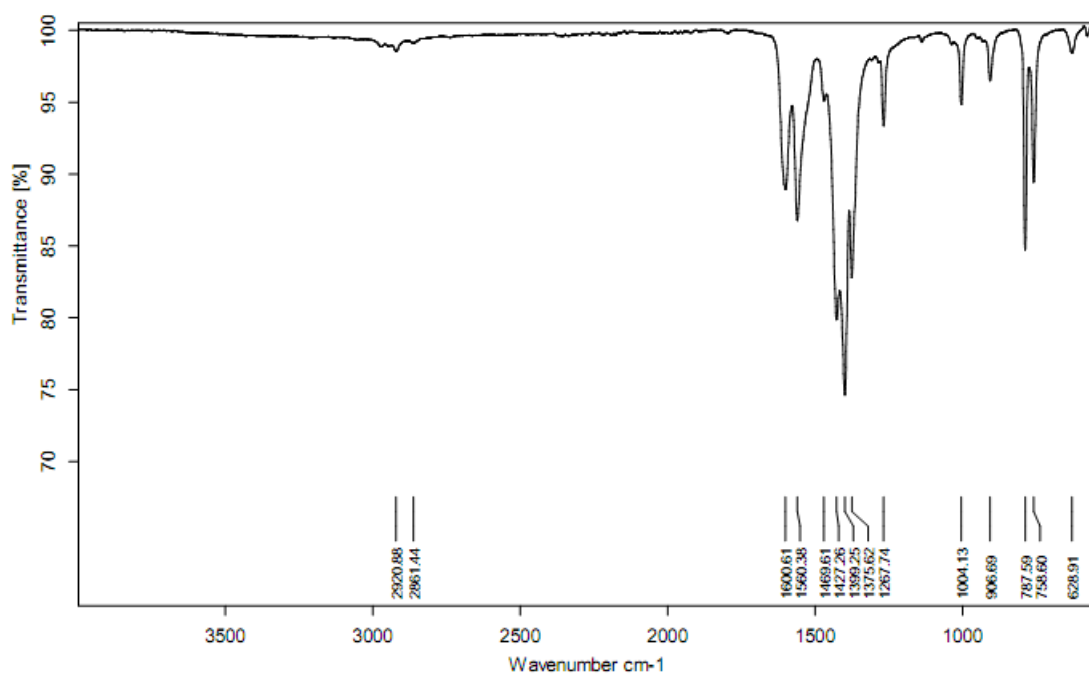


Fig. S5 IR spectrum of $[\text{Zn}_4\text{O}(\text{Me}_4\text{BPDC})_3], \mathbf{2}$ (degassed).

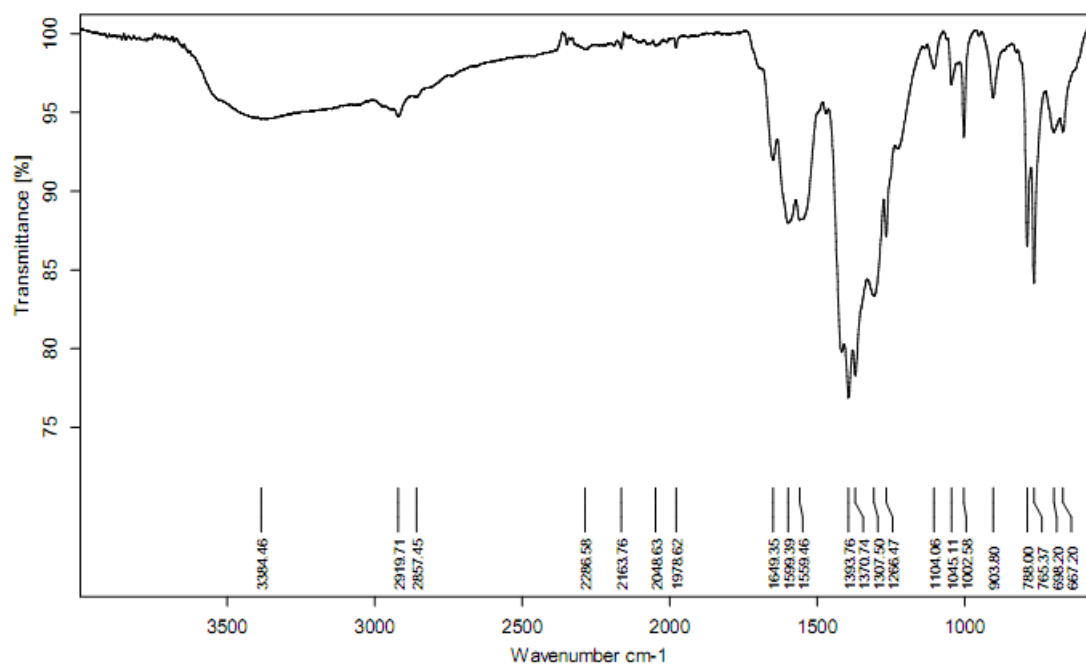


Fig. S6 IR spectrum of $[\text{Cu}_2(\text{Me}_4\text{BPDC})_2] \cdot 9 \text{ DMF}$, **3** · 9 DMF (as synthesized).

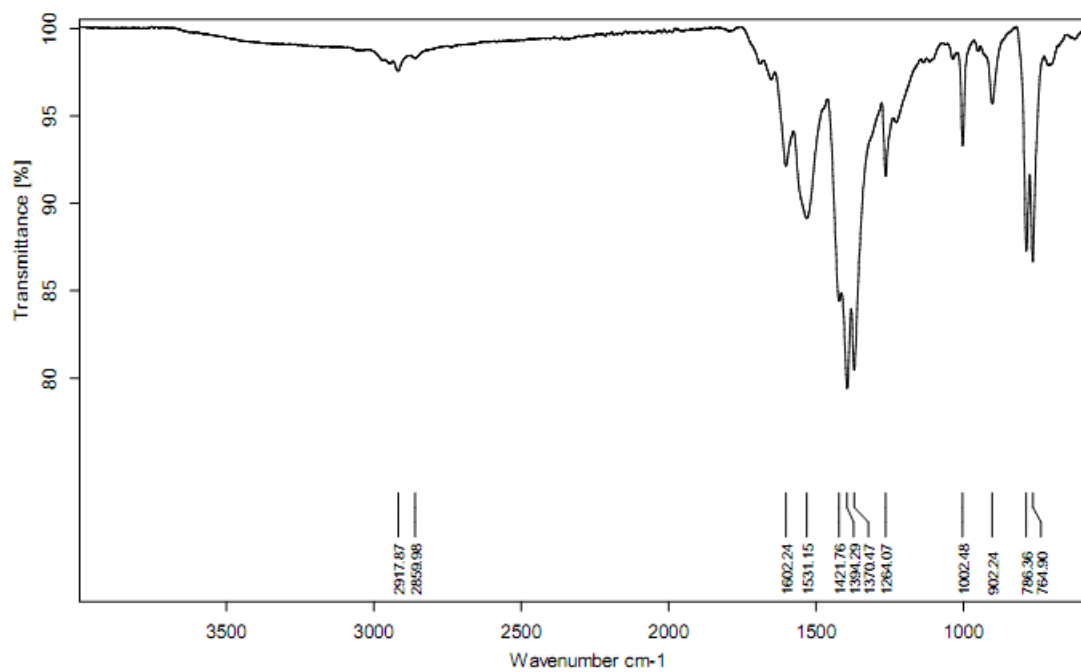


Fig. S7 IR spectrum of $[\text{Cu}_2(\text{Me}_4\text{BPDC})_2]$, **3** (degassed).

Table S2 Assignments of IR data for the as synthesized and activated samples **2** and **3**.

2 · 9 DMF	2	3 · 9 DMF	3	Assignments
~3300 (w, vbr)		3384 (w, vbr)		ν N _{amide} H DMF
2919 (vw)	2921 (vw)	2920 (vw)	2918 (vvw)	w; ν C _{Ar} H w; ν C _{aliph} H
2861 (vw)	2861 (vw)	2857 (vw)	2860 (vvw)	
1666 (m)		1649 (m)		ν_{as} C=O [DMF]
1601 (s)	1602 (s)	1599 (m)	1602 (m)	ν_{as} CO ₂ ⁻
1559 (s)	1560 (s)	1559(m)	1531(m)	ν_{as} CO ₂ ⁻
1423 (s)	1427 (s)	1422 (s)	1421 (s)	ν Ph
1395 (s)	1399 (s)	1394 (vs)	1391 (s)	ν_s CO ₂ ⁻
1371 (s)	1376 (s)	1371 (vs)	1370 (s)	ν_s CO ₂ ⁻ , ν CH [(CH ₃)NCHO]
		1308 (s)		
1266 (m)	1268 (m)	1266 (m)	1266 (m)	ν Ph(?)
1095 (w)	-	1104 (w)		DMF (?)
		1045 (m)		
1003 (w)	1004 (w)	1002 (m)	1002 (m)	γ C _{Ar} H, DMF
907 (w)	907 (w)	904 (w)	902 (w)	
789 (s;	788 (s)	788(s)	786(s)	γ C _{Ar} H
760 (s;	759 (s)	765 (s)	762 (s)	δ CO ₂ ⁻
663(vw)	629 (vw)	698 (m)		
628 (vw)		667 (m)		

ν - stretching; δ - in-plane deformation; γ - out-of-plane deformation;

v - very; s - strong; m - medium; w - weak; sh - shoulder; br - broad;

subscripts: as - asymmetric; s - symmetric

The assignment was done according to [1].

- [1] H.T.Varghese, C.Y. Panicker, D. Philip, K. Sreevalsan, V. Anithakumary, Spectrochim. Acta Part A: Molec. Biomolec. Spectr. 68 (2007) 817-822.

Pore size distribution according to DFT calculations (N₂ sorption data)

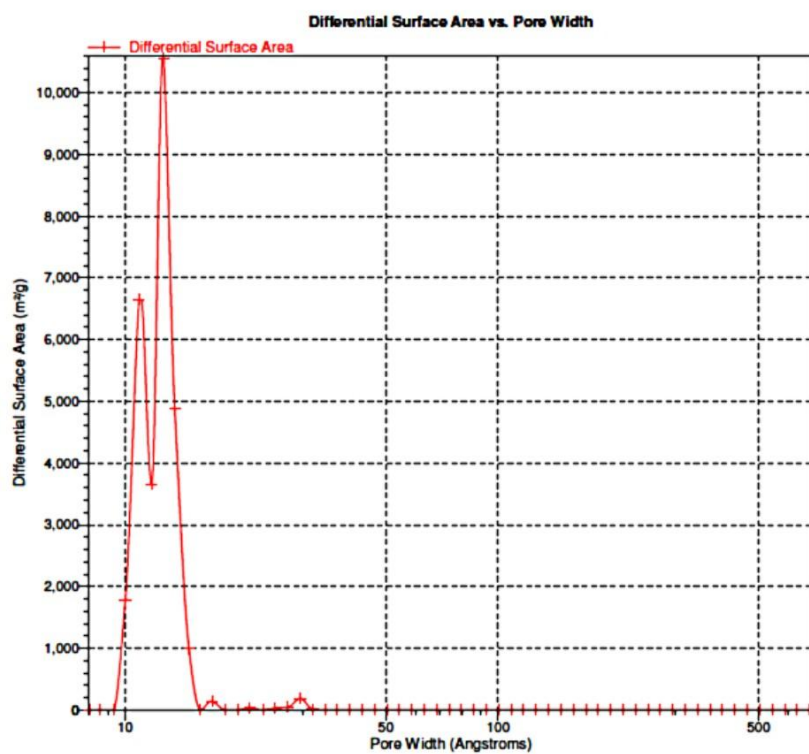


Fig. S8 DFT calculations for **2** (differential surface area (m² / g) versus pore width (Å))

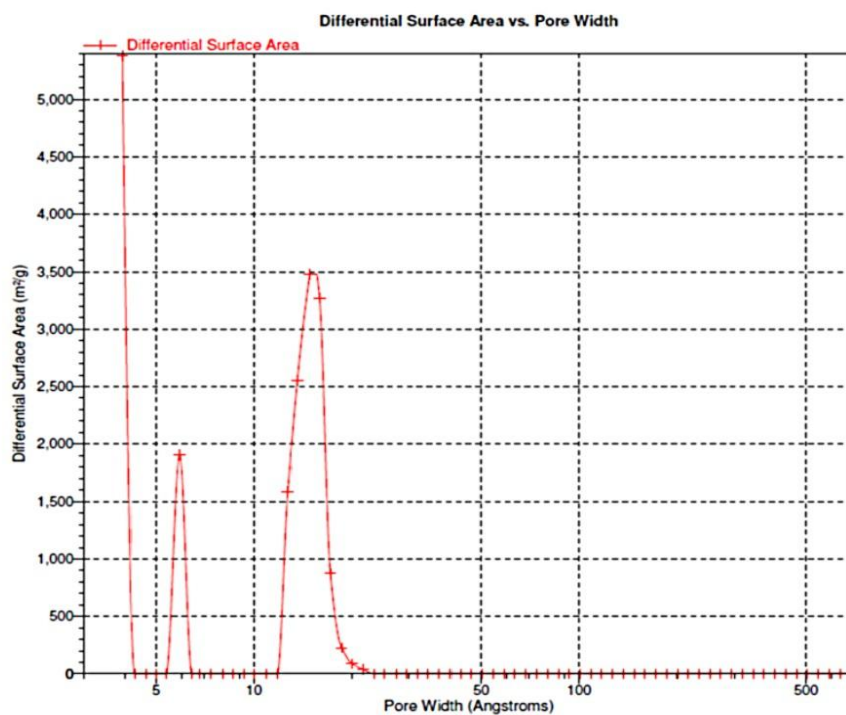


Fig. S9 DFT calculations for **3** (differential surface area (m² / g) versus pore width (Å))

Powder X-ray diffraction patterns

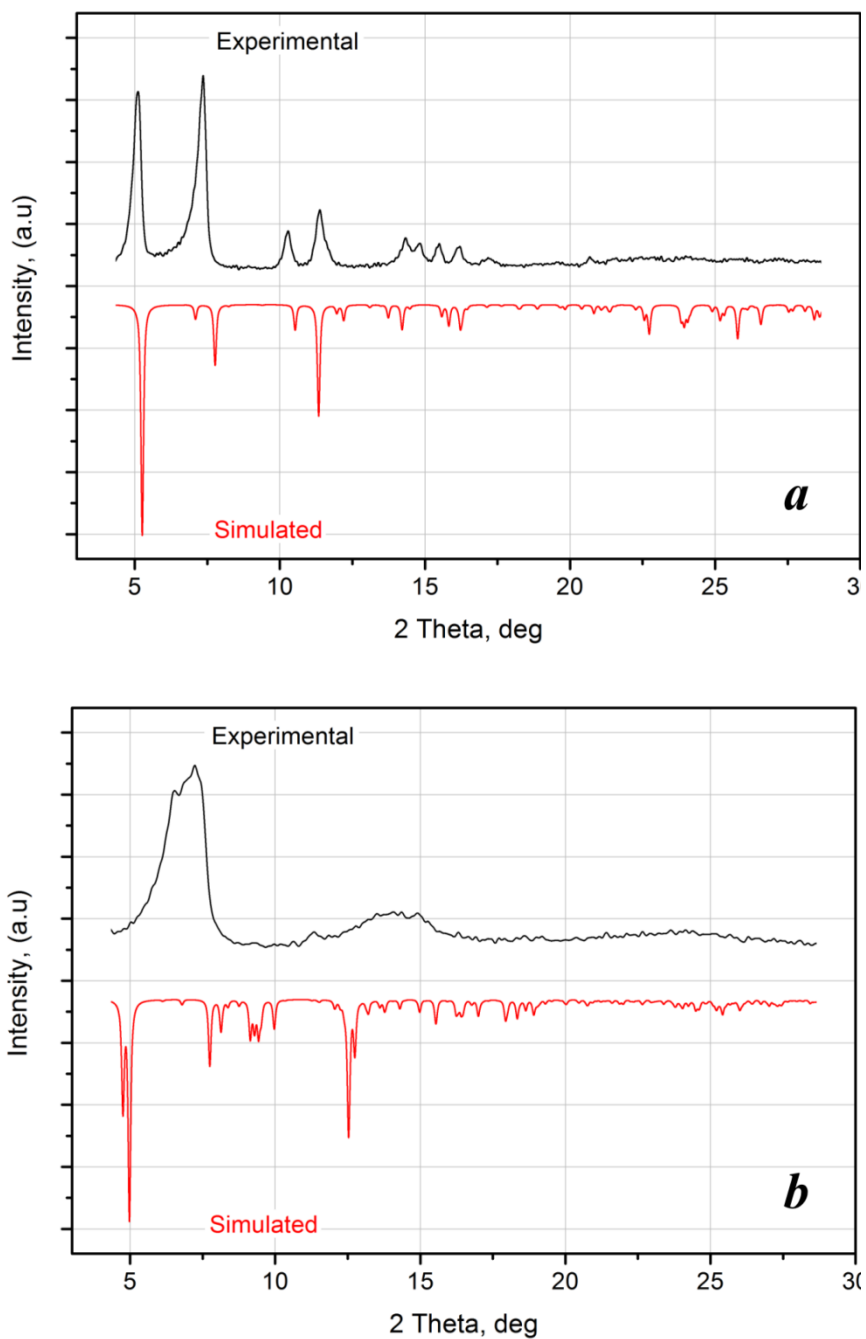


Fig. S10 Powder X-ray diffraction patterns of **2** (a) and **3** (b) after degassing, compared with the simulated diffractogram based on the data of the single crystal XRD structural experiment (all the solvent atoms were removed prior to simulation).

Approximate heat of adsorption (HoA) dependence on adsorbed quantities of CO₂ and CH₄ for 2 and 3^I

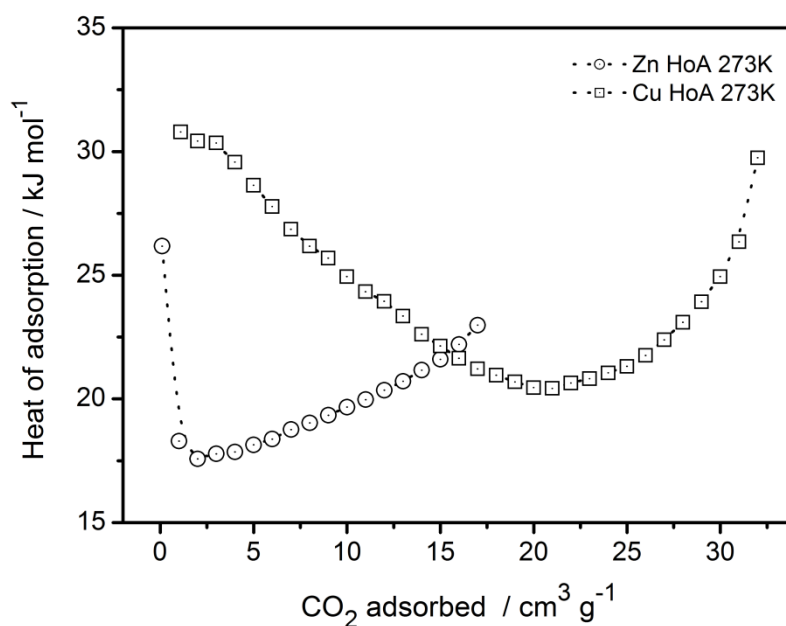


Fig. S10 HoA of CO₂ for the samples 2 (Zn) and 3^I (Cu), 273-293K.

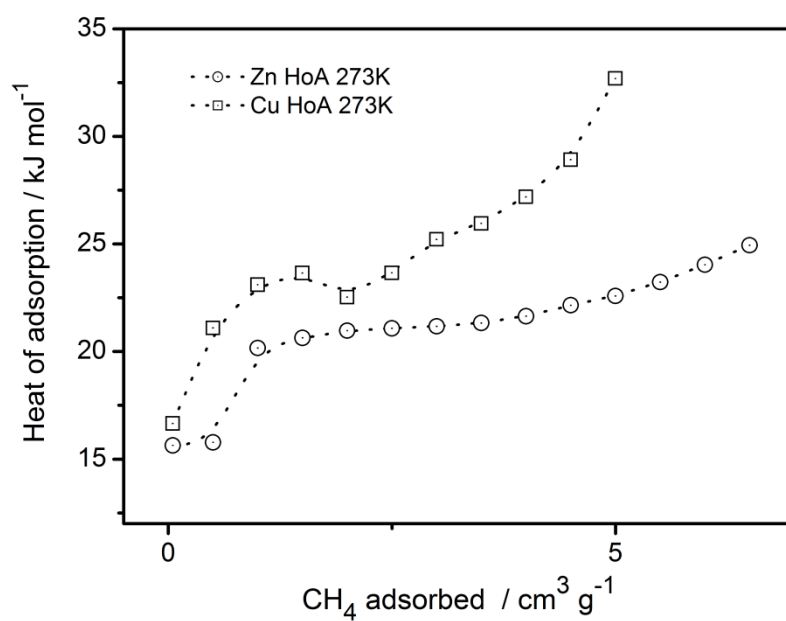


Fig. S11 HoA of CH₄ for the samples 2 (Zn) and 3^I (Cu), 273-293K.